sciendo

POLISH MARITIME RESEARCH 3 (115) 2022 Vol. 29; pp. 11-20
10.2478/pomr-2022-0022

CFD OPTIMISATION OF THE LONGITUDINAL VOLUME DISTRIBUTION OF A SHIP'S HULL BY CONSTRAINED TRANSFORMATION OF THE SECTIONAL AREA CURVE

Marek Kraskowski *
Maritime Advanced Research Centre S.A., Poland

* Corresponding author: *marek.kraskowski@cto.gda.pl (M. Kraskowski)*

ABSTRACT

The paper presents a proposal for a formalised approach to hull shape optimisation with respect to total resistance, by fine-tuning longitudinal volume distribution. An algorithm for automated modification of the hull is presented, allowing for varying the sectional area distribution with a negligible influence on the resulting displacement. Computational fluid dynamics (CFD) solver STAR-CCM+ and computer computer-aided design (CAD) software NX were used to search the optimal volume distribution of selected parent shapes, with respect to total resistance. The bow part and the aft part were optimised separately. The resulting resistances of the selected optimal shapes were then verified by means of scale model tests, realised in the towing tank at the Maritime Advanced Research Centre (CTO) S.A. A noticeable gain in total resistance was achieved and confirmed by experimental tests. The proposed approach seems to be a promising method for relatively quick parametric optimisation of the designed hull shapes; it is also applicable for generic CFD optimisation studies.

Keywords: parametric optimisation, CFD, model tests, resistance, wave pattern

INTRODUCTION

The trends observed in modern research focused on experimental and computational ship hydromechanics, reflect new possibilities provided by advanced software, high-performance computers and advanced control systems applied in experimental setups. Examples of state-of-the-art experimental techniques were presented by Lu et al. [1] and Bielicki [2]. In computational fluid dynamics, the focus is on simulating fully nonlinear dynamics [3] and on effective shape optimisation [4]. In terms of computational analyses, the last two decades have witnessed a revolution in the feasibility of computational fluid dynamics (CFD) analyses in engineering applications. In the early 2000's, viscous flow analyses were carried out by full-time researchers, for relatively simple objects and with the use of coarse block-structured meshes. However, objects of arbitrary complexity can now be easily analysed by engineers. This progress has mainly been made possible due to the development of computers, automated unstructured meshing, and the ability to handle complex geometries and user-friendly graphic interfaces. Attempts to formalise the optimisation of analysed geometries were also made from the very beginning of the solvers development. Initially, the multi-variant analyses were possible with the use of potential codes [5] and for 2D cases [6]. Later on, the growing power of computers and efficiency of computer-aided design (CAD) software allowed for parametric optimisation of actual 3D geometries with the use of Reynolds-Averaged Navier-Stokes

(RANS) solvers. An example of the effective optimisation of a parametrised hull shape was presented by Gundelach [7]. His approach to hull modelling can be referred to as a Fully Parametric Model (FPM), in which the CAD surface is based on Non-Uniform Rational B-Spline (NURBS) curve surfaces defined from scratch. A foundation for this approach was prepared by Nowacki [8] and Harries [9,10]. Examples of the successful application of fully parametric models for hull shape optimisation were presented by Biliotti et al. [11], Han et al. [12] and Brenner et al. [13]. In order to make the optimisation process more efficient, surrogate models are also used [14]. However, parametrisation of a free form shape, like a ship's hull, usually requires careful selection of the regions to be modified and advanced coding, which makes the CAD preparation time-consuming, and so this approach is not very feasible in engineering practice. An alternative approach is the *a posteriori* transformation of an existing CAD file, which makes the possibilities for modification very limited, but the parametrisation itself can be realised relatively quickly [15]. Examples of such an approach were presented by Peri and Campana [16], Perez and Clemente [17] and Choi [18]. This paper also presents a variant of this approach; the optimisation is focused on finding the optimum balance between the angle of the ends of the waterplane and the fairness of the shoulders. This kind of optimisation is applicable for fine-tuning of pre-optimised shapes with no major faults. An example of the application of the proposed approach, to a selected shape, and the experimental verification of the results is presented.

PARENT HULL SHAPE

The presented analyses were carried out for the INSEAN 7000 DWT Tanker. Its shape is presented in Fig. 1 and its basic features are presented in Table 1.

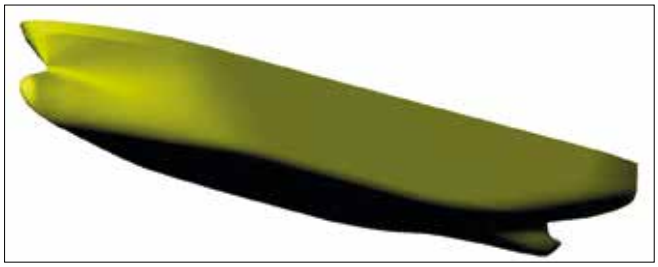

Fig. 1. Parent hull shape

Tab. 1. Basic features of the parent hull shape

Length between perpendiculars	L_{PP} [m]	94.00
Breadth	B [m]	15.40
Draught	T [m]	6.00
Displacement	∇ [m^3]	6827
Wetted surface area	S [m^2]	2249
Block coefficient	C_B [–]	0.786
Design speed	V [kn]	14
Froude number	F_n [–]	0.237

POSSIBLE APPROACHES TO SHAPE PARAMETRISATION

Parametrisation of the CAD geometry consists of defining the dependencies between the locations of points and angles of curves etc. by introducing expressions, such that changing the value of one or more global variables modifies the whole geometry. This can be explained by the simple example of a cube. If the properties of this solid are not known, its unequivocal definition in a Cartesian coordinate system requires the specification of 24 figures, i.e. three coordinates for each of the eight corners of the cube. However, if we know the dependencies between the coordinates of the cube corners, we can define and modify its geometry by giving just one figure, i.e. the length of one side.

Two important observations can be made on the basis of this example:

1. Although the modification of the parametrised geometry is very fast, much more work is required to prepare the CAD definition, due to the need to define the dependencies between selected geometric features of the object.
2. Parametric definition of the object loses flexibility in introducing the modifications, e.g. changing the form of the regular cube into an arbitrary cuboid is not possible with parametric definition, while it is straightforward with a standard definition.

Several attempts have been made to achieve effective hull form parametrisation; it was found that two general approaches can be distinguished:

1. Building the parametrised hull definition from scratch, i.e. defining points, curves and surfaces so as to match the required basic shape, and then defining the dependencies between the locations of the points, curve angles etc. to enable efficient modifications.
2. Defining the control points and planes so as to control the surface provided in the form of a CAD exchange file, e.g. IGES, and then defining the dependencies between the locations of control points and planes to enable efficient modifications.

The 'pros and cons' of the described approaches can be easily pointed out, assuming that the task to be realised consists of optimising the initial proposal of the shape provided by the customer.

1. Building the parametrised definition from scratch.

Advantages:

+ allows much more accurate control of the details of the geometry;
+ provides full flexibility in deciding which regions will be modified and how.

Disadvantages:

– when the definition is relatively simple, i.e. based on a small number of points and curves, it is almost impossible to accurately match the basic shape required;
– on the other hand, if the shape is to be reproduced accurately, the complexity of the definition increases

dramatically, which makes it less useful in introducing modifications;
– defining the hull from scratch always requires a relatively long time, while the fast exchange of proposals is especially important at an early stage of the contract.

2. Defining the control points and planes allowing transformations of the existing shape.

Advantages:
+ full match between the basic shape and its parametrised definition;
+ the process of parametrisation is fast and easy.

Disadvantages:
– considerably limited control of the details of the geometry.

Both approaches were attempted and the results are presented in the following sections.

HULL PARAMETRISATION

As mentioned in the introduction, the selected approach is based on the *a-posteriori* transformation of existing hull surface definition; an attempt to model the shape with a fully parametric definition turned out to be inefficient. It was either very hard to obtain the required consistency with the parent shape, or the definition became extremely complex. Parametric transformation of the existing geometry was realised using the Global Shaping feature of the NX software. NX CAD is a very generic environment, designed for integrated computer aided engineering. It contains CAD, CAM, CFD, FEM and other tools; in the presented work, only the CAD module was used. Global Shaping is a feature dedicated to manipulating the features of an object imported as an external geometry file. The method of transformation is explained on the basis of Fig. 2 and can be described as a formalised global shaping.

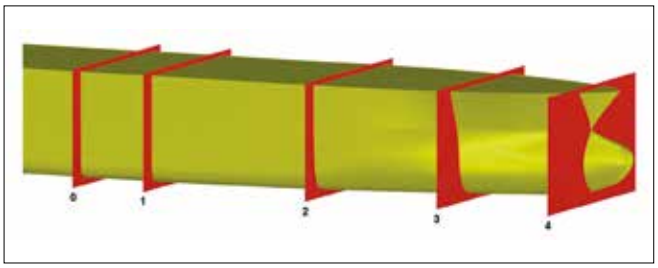

Fig. 2. Transformation with the use of control planes

An arbitrary number of control points is assigned to the transformed region. In the presented case, the transformation is applied to the region between the mid-ship section and the fore perpendicular. The locations of the points located at the ends of the region (0 and 3 in the presented case) remain unchanged. All of the control points located between them (1-2) can be shifted arbitrarily, which results in the continuous shift of the hull sections in the region between points 0 and 3. The resulting shift in individual sections, relative to their initial position, is evaluated using the Bézier curve formulation. This formulation is explained in detail below.

Let us define the vector of the initial locations of the control points:

$$X_{BASE} = [x_0 \;\; x_1 \;\; x_2 \;\; x_3 \;\; x_4]. \tag{1}$$

The transformation is realised by shifting the control points to new locations:

$$X_{TR} = [x_{0\_TR} \;\; x_{1\_TR} \;\; x_{2\_TR} \;\; x_{3\_TR} \;\; x_{4\_TR}]. \tag{2}$$

In the presented case, $x_0 = x_{0\_TR}$ and $x_4 = x_{4\_TR}$; however, in a generic case, this does not necessarily hold true.

The difference between the initial and transformed location of the control points is denoted as:

$$\Delta X = X_{BASE} - X_{TR} = [\Delta x_0 \;\; \Delta x_1 \;\; \Delta x_2 \;\; \Delta x_3 \;\; \Delta x_4]. \tag{3}$$

Our goal is to evaluate the shift of an arbitrary point located between x_0 and x_4, based on the values of ΔX. For this purpose, we introduce the parameter $t \in [0,1]$ and parametrise the length of the transformed region, so that x_0 corresponds to $t = 0$ and x_4 corresponds to $t = 1$. The shift of the arbitrary point between x_0 and x_4 is evaluated using the formula:

$$dx(t) = \sum_{i=0}^{n} \Delta x_i B_i^n(t) \tag{4}$$

where are so-called Bernstein polynomials [9] and defined as:

$$B_i^n(t) = \begin{cases} \binom{n}{i} t^i \, (1-t)^{n-i} & \text{for} \quad i = 0 \ldots n \\ 0 & \text{for} \quad i < 0, \, i > n \end{cases}. \tag{5}$$

Let us now present an example of shape transformation based on 4 control points (n = 3). The graph below (Fig. 3) shows the form of Bernstein polynomials for i = 0....4.

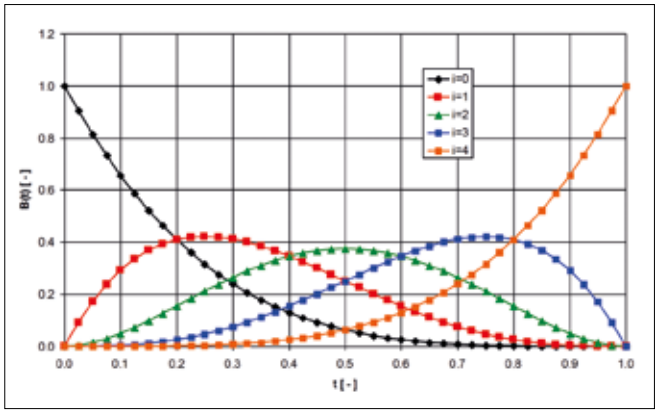

Fig. 3. Bernstein polynomials

The formulation of the transformation results show that the locations of the control points have no influence on the transformation results; it is only the number of control points which affects the transformation form. The control points are, thus, evenly distributed along the modified region, which results from the technical requirements of the applied NX software (we use mid-ship as the zero point and fore perpendicular as the end point, x = 47 m):

$$X_{BASE} = [0 \;\; 11.75 \;\; 23.50 \;\; 35.25 \;\; 47]. \tag{6}$$

We then introduce the following transformation based on a single parameter p (values of the vector ΔX):

$$\Delta X = [0 \quad -p \quad -p \quad a \cdot p \quad 0]. \tag{7}$$

According to Eq. (7), the result of shifting three control points on the transformation of the sectional area curve of the bow part is shown in Fig. 4 (modified – red). The contribution of subsequent control points, as well as the resulting shift dx, is presented in the second graph.

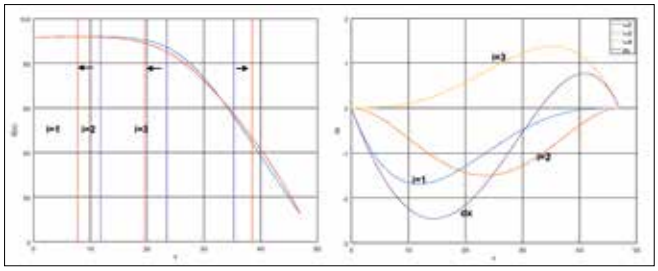

Fig. 4. Using Bernstein polynomials for shape transformation

The coefficient a is a constant which is used to calibrate the transformation procedure, so that the displacement volume remains constant within a considered range of variation of parameter p. The range of p is limited by the software requirements, i.e. the control planes must not swap places along the hull after transformation; in other words: if the x coordinate of plane i is larger than the x coordinate of plane i-1 before transformation, it must still be larger after transformation (this is not a limitation of the formulation itself). On the other hand, the transformed shape for extreme values of parameter p must still fit the ship-shape canon; however, this criterion has no mathematical formulation, it is only based on designer experience and intuition. The procedure for selecting the range of p and value of a can be described as follows:

- select an interval (usually symmetrical) of parameter p which meets the mentioned criteria; in the presented example, the range is from -4 to 4;
- set the value of p to the minimum of the assumed interval and set the value of a to 1;
- use the trapezoid rule to integrate the sectional area curve and compare the displacement volume before and after the transformation; vary the coefficient a to obtain a match;
- repeat the procedure for the maximum value of parameter p, using the value of a found in the previous step; in the presented example, a match was achieved without further iteration.

Using a MATLAB routine for the transformation and integration allows the correct value of a to be found in just a few steps, in a guess-and-check manner. In the presented example, a constant value of a allowed a constant displacement to be maintained with an accuracy of 0.2 m^3, i.e. 0.006%.

The longitudinal centre of buoyancy (LCB) of the ship is not directly controlled in the described procedure. In the presented example, changing the parameter p between –4 and 4, results in shifting the centre of volume of the fore part by 0.113 m, which results in shifting the LCB of the ship by 0.057 m (0.06% of L_{pp}). If such a change in LCB is acceptable, as assumed in the presented study, the fore part and the aft part can be optimised independently. If not, then the aft part must be transformed in parallel with the fore part, so as to compensate any change in LCB. The resulting modifications of the sectional area curve for extreme values of parameter p are presented in Fig. 5.

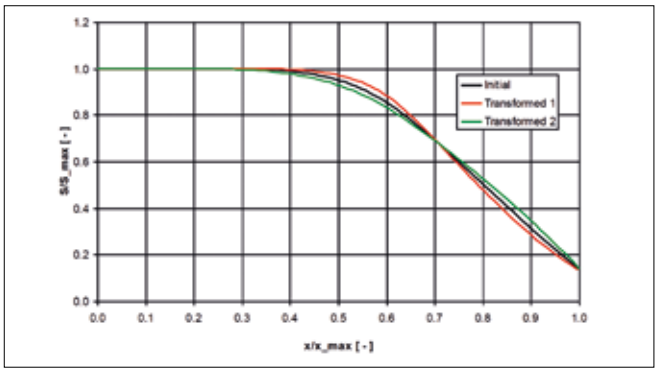

Fig. 5. Considered range of modifications of the longitudinal volume distribution

The described method of parametrised hull transformation is quite similar to the well-known Lackenby transformation [20], in the sense that existing hull sections are moved to new locations. The features of the method, in comparison with the studies presented by the cited authors, are as follows:

- shape is controlled by just one parameter;
- applied constraints imply that all of the modifications generated during the optimisation process are allowable (constant displacement volume);
- a very small number of cases are analysed in order to find the optimum.

The method is also easy to implement, using the commercial NX software in the presented study. On the other hand, its drawback is that, at the moment, it is dedicated to optimise a single geometric feature of the hull.

COMPUTATIONAL MODEL

The resistance for subsequent variants of the parent shape was computed with the use of STAR-CCM+ solver. The computations were carried out at full scale. The CFD solver was coupled with the NX CAD software and the computational procedure was executed in the following manner:

- a table of the required range of parameter p to be analysed, was pre-defined and imported to the CFD solver;
- the CFD solver managed the process by sending the command to the CAD software at the beginning of each analysis, to execute another modification;
- the modified shape was imported to CFD solver, which executed the re-meshing and analysis.

This procedure is presented in the form of the flowchart in Fig. 6.

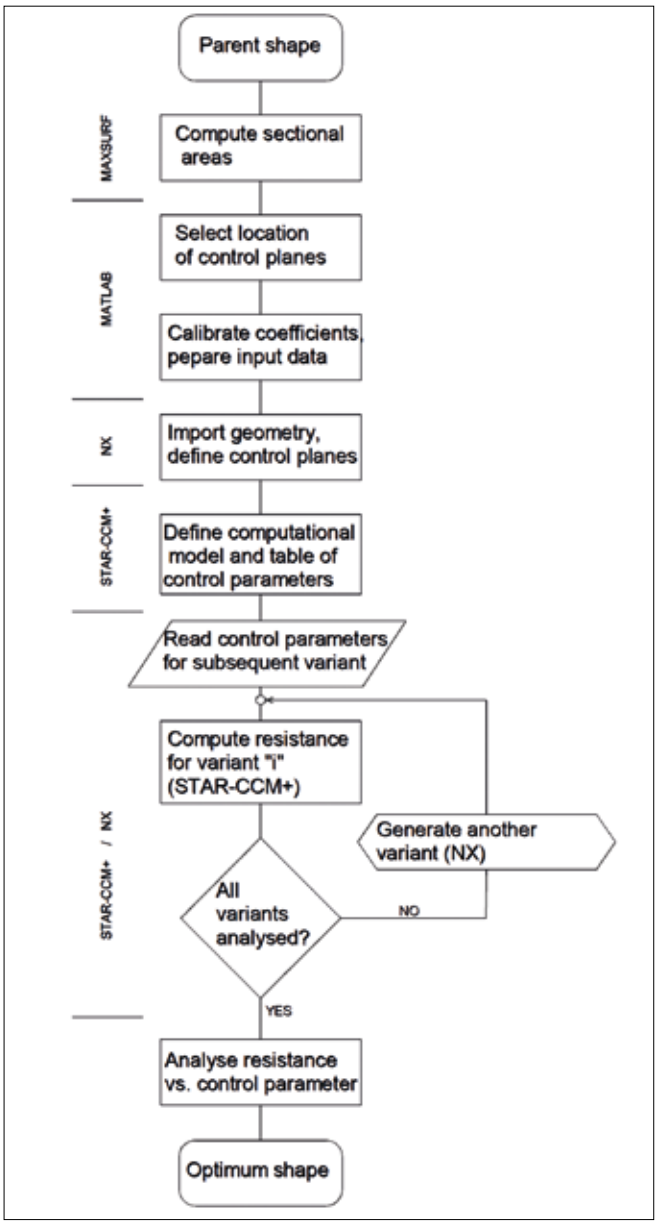

Fig. 6. Optimisation procedure - flowchart

As the low computational time is of high priority, and the focus was primarily on differences in resistance rather than absolute values of the resistance, a relatively coarse mesh was used and the dynamic trim and sinkage were neglected. Initial trim and draught were adjusted, based on the computations for the parent shape, and remained unchanged for all other variants, assuming that their variation would be small, due to constant displacement and LCB. The number of mesh cells for the optimisation process was 1.9 x 10^6. Computations for variable mesh density confirmed that increasing the number of cells above this value does not influence the tendencies revealed in the optimisation process. The boundaries of the rectangular domain were located as follows: inlet - 2L upstream of the bow, outlet - 2L downstream of the stern, bottom - 2L below the hull base line, top 1L above the hull base line, lateral wall - 2L from the hull symmetry, where L is the overall ship length. The computational domain is presented in Fig. 7.

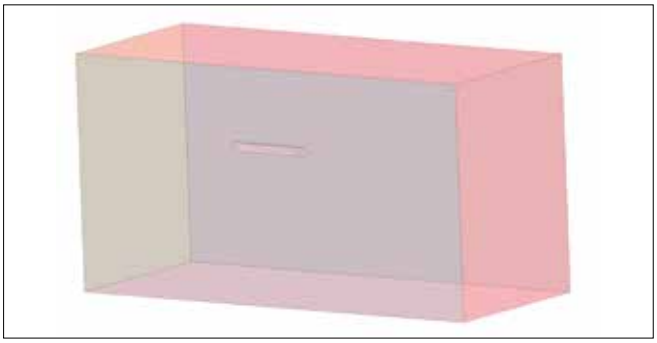

Fig. 7. Computational domain size

The types of boundary condition are as follows:
– upstream, top, bottom and side walls of the domain: prescribed velocity components and volume fraction of water;
– downstream: prescribed pressure;
– hull: no-slip wall.

The wave damping zone was used in the region close to the domain boundaries in order to speed up convergence by preventing the wave reflections inside the domain.

The settings of the computational model were as follows:
– free surface treatment: multiphase flow (Volume of Fluid);
– implicit unsteady model;
– turbulence model: k-epsilon;
– time step: 0.02 s;
– 5 outer iterations per time step.

The visualisations of the mesh are presented in Fig. 8 and Fig. 9.

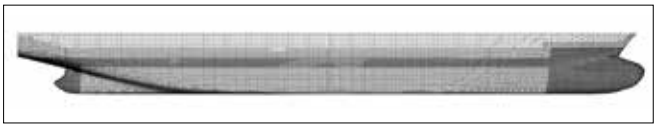

Fig. 8. Computational mesh - hull surface

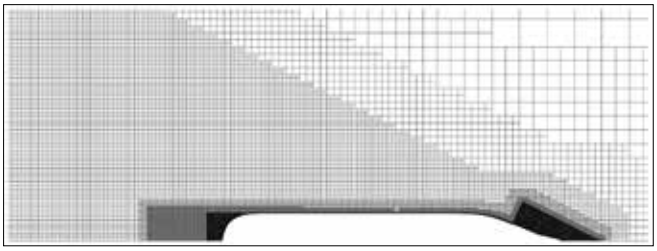

Fig. 9. Computational mesh - free surface region

The resulting y+ values on the hull surface are presented in Fig. 10. Relatively large values of y+ (above 100) enforce the application of wall functions.

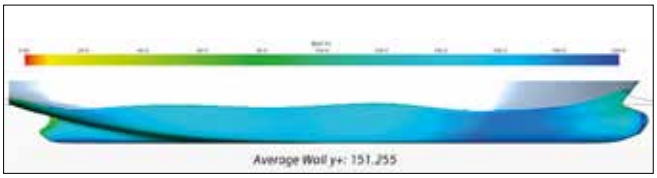

Fig. 10. Wall y+ on the hull surface

Convergence of the continuity equations and convergence of the resistance value for the selected case are presented in Fig. 11 and Fig. 16, respectively.

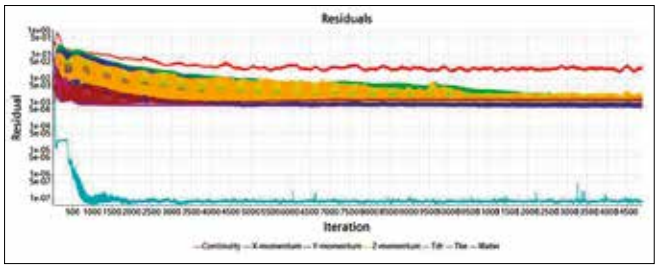

Fig. 11. Residuals

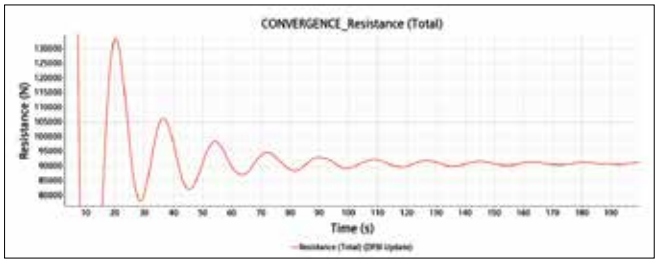

Fig. 12. Convergence of the resistance

RESULTS OF BOW PART OPTIMISATION

The bow part optimisation, with respect to resistance, was carried out in two steps. The first step was the optimisation of the longitudinal volume distribution between the mid-ship section and the fore perpendicular; the second step was the optimisation of the bow bulb length. Location of the control points, for the optimisation of longitudinal volume distribution, is presented in Fig. 13 (three variable control points).

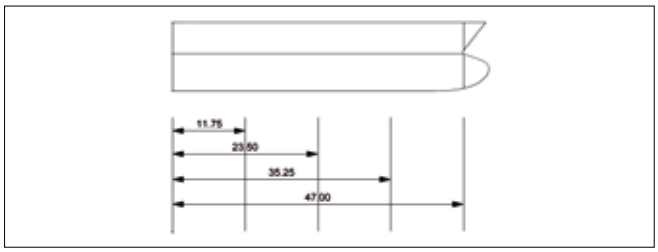

Fig. 13. Location of the control points for the bow part

Location of the control points for the optimisation of bow bulb length is presented in Fig. 14.

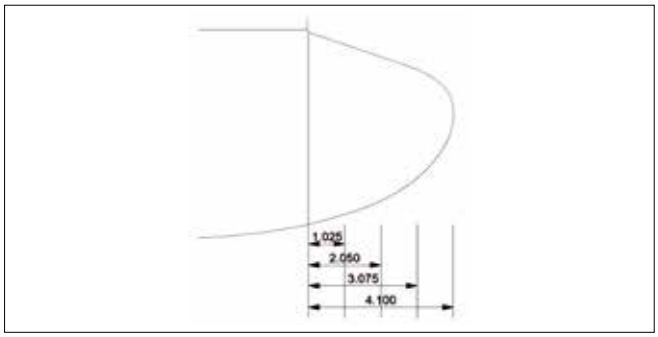

Fig. 14. Location of the control points for the bow bulb

The search for the optimum longitudinal volume distribution started with a quick analysis of global tendency. Five values of parameter p were used to generate the population of shapes: -4, -2, 0, 2 and 4 (5 variants), where $p =$ 0corresponds to parent shape. The resulting relative resistance values are presented in Fig. 15.

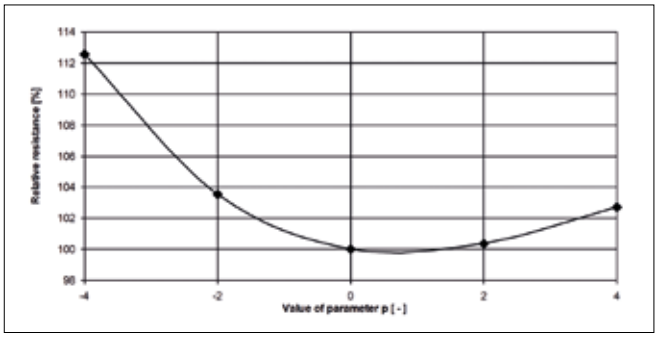

Fig. 15. Relative resistance for five variants of the bow part

The influence of the modifications on the bow pattern for two extreme variants as well as the optimal variant is presented in Fig. 16.

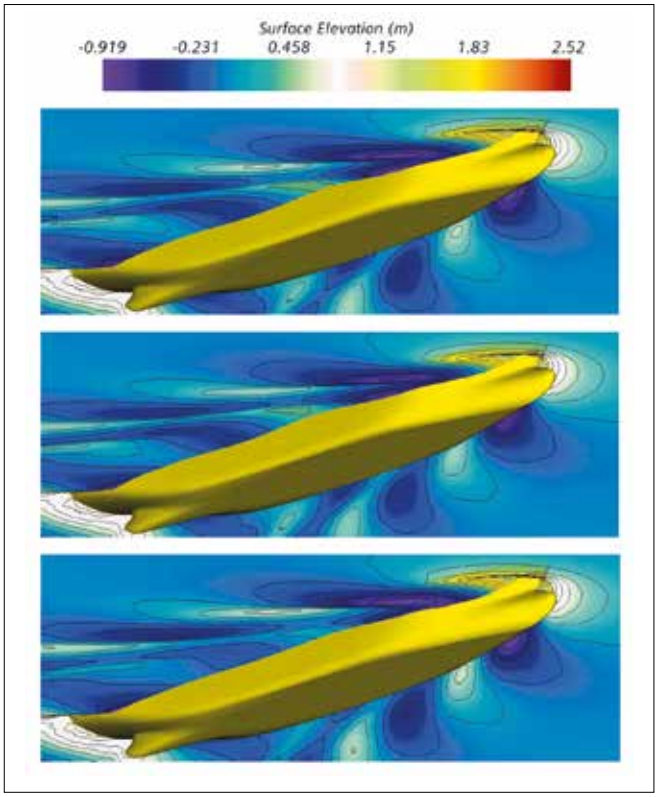

Fig. 16. Optimisation of the bow part - wave pattern: lowest waterplane entrance angle (top), optimum (middle) and fairest shoulder (bottom)

The quantitative results show that the computer resistance is lowest for the parent shape, i.e. no improvement was achieved in the first attempt. However, the shape of the curve suggests that the actual minimum resistance should be expected for the value of parameter p between 0 and 2. Thus, the computations were continued for three more variants of hull shape, corresponding to the values of parameter p equal to 0.4, 0.74 and 1.0. The results are presented in Fig. 17.

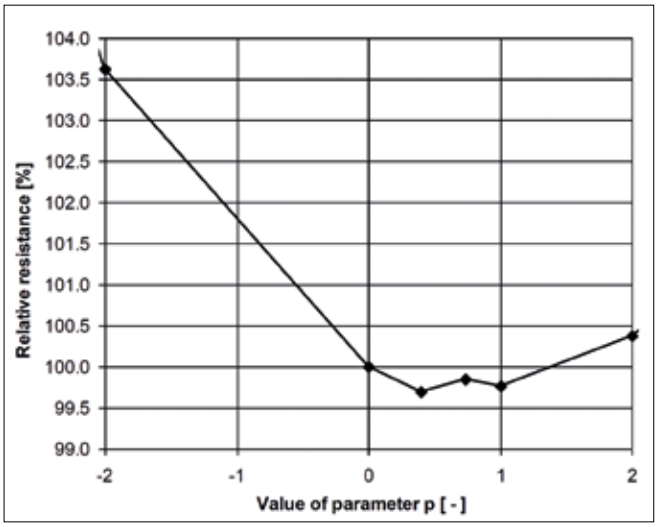

Fig. 17. Analysis of relative resistance for refined range of parameter p

A slight reduction in resistance was observed; however, it was almost negligible (approximately 0.25%).

The next step of the optimisation of the bow part was the optimisation of the bulb length. The length was changed within the range 4.1-6.1 m (the upper limit was selected arbitrarily). In the case of bulb optimisation, the influence of its size on total displacement volume was neglected; the actual increase of volume for the longest bulb was 16 m^3, which corresponds to 0.2% of the total volume of the parent shape. A change in LCB also occurs, equal to 0.12% of L_{PP}. The location of the control points presented in Fig. 14 was changed, proportionally, i.e. the bulb was transformed by uniform 'stretching'. Five variants of the bulb were analysed. The resulting relative resistance values are presented in Fig. 18 (100% now corresponds to initial bulb length).

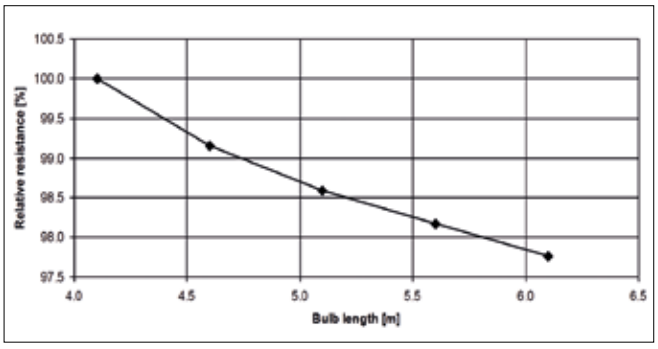

Fig. 18. Relative resistance as a function of bulb length

As can be seen, the resistance decreases monotonically with increasing bulb length. The total reduction of resistance due to optimisation of the bow part achieved is 2.54%, which is noticeable from the point of view of fuel consumption.

The influence of the bow bulb modifications on the wave pattern are presented in Fig. 19.

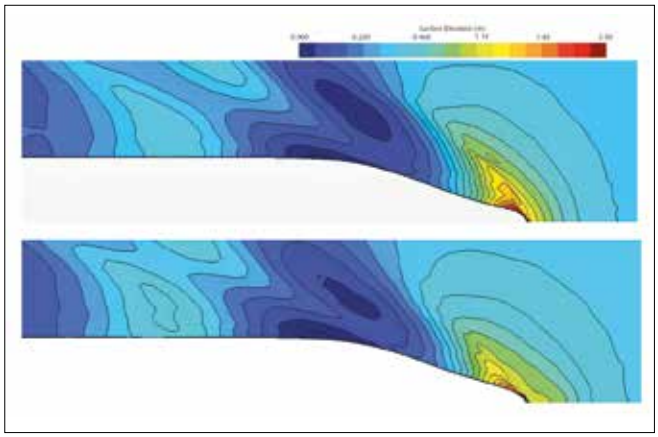

Fig. 19. Optimisation of the bow bulb - wave pattern: initial bulb (top) vs. optimised bulb (bottom)

Comparison between the bow parts of the parent shape and the optimised one is presented in Fig. 20.

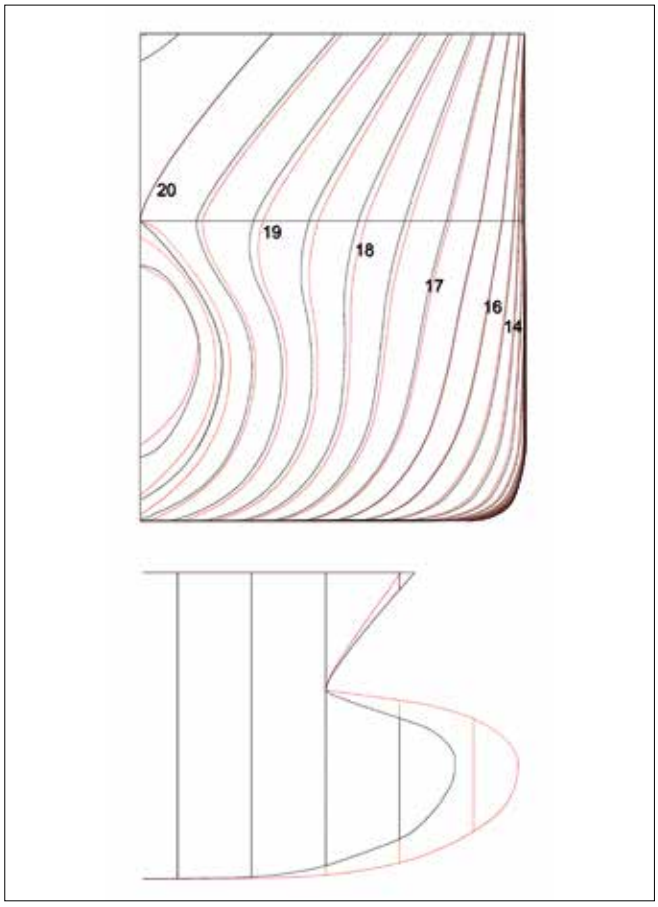

Fig. 20. Bow part - parent shape (black) vs. optimised one (red)

RESULTS OF STERN PART OPTIMISATION

Optimisation of the stern part only comprised the optimisation of the longitudinal volume distribution. The location of the control points is presented in Fig. 21 (four variable control points).

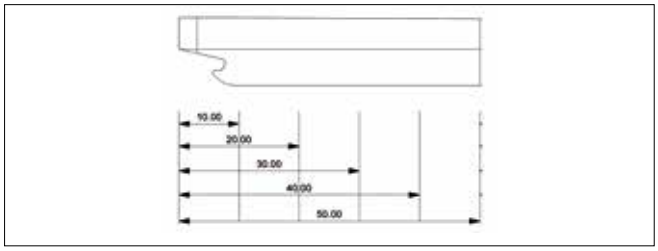

Fig. 21. Location of the control points for the stern part

In the case of a stern part, there are four intermediate control points: the values of the vector

$$\Delta X = [0 \quad -p \quad -p \quad a \cdot p \quad a \cdot p \quad 0]. \tag{8}$$

The considered values of parameter p were: -3, -1, 0, 1, 3, 5 and 6 (seven variants), where $p = 0$ corresponds to the parent shape. The relative resistance for the resulting hull shape variants is presented in Fig. 22.

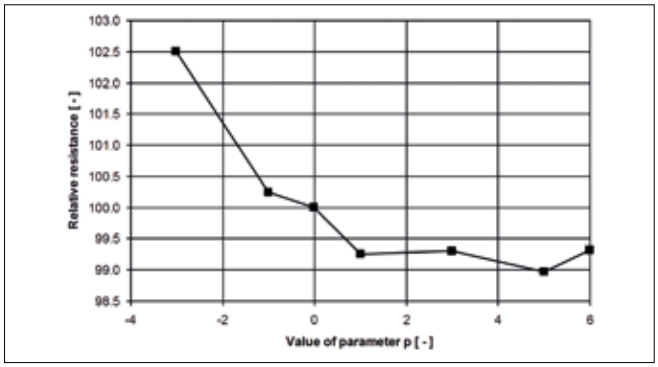

Fig. 22. Relative resistance for seven variants of the stern part

In the case of the stern, total resistance was reduced by 1.03%, according to CFD results. The influence of the stern part modifications is presented in Fig. 23.

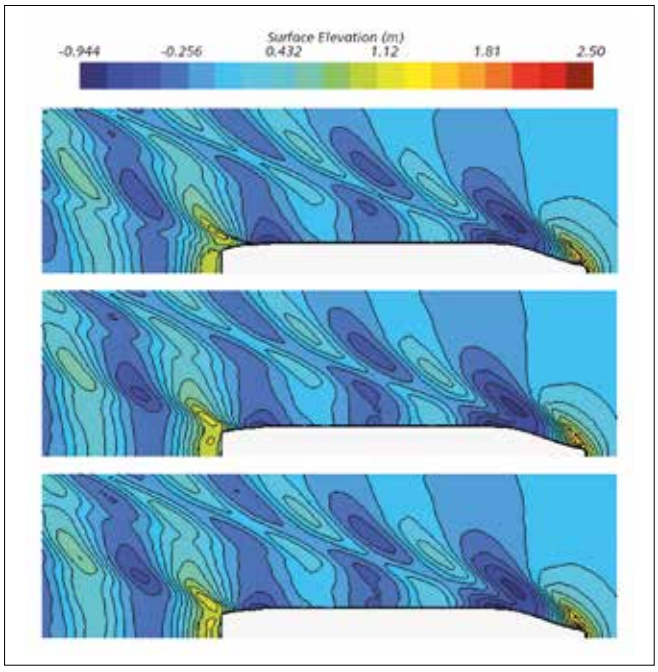

Fig. 23. Optimisation of the bow part - wave pattern: lowest waterplane entrance angle (top), optimum (middle) and fairest shoulder (bottom)

Comparison between the aft parts of the parent shape and the optimised one is presented in Fig. 24.

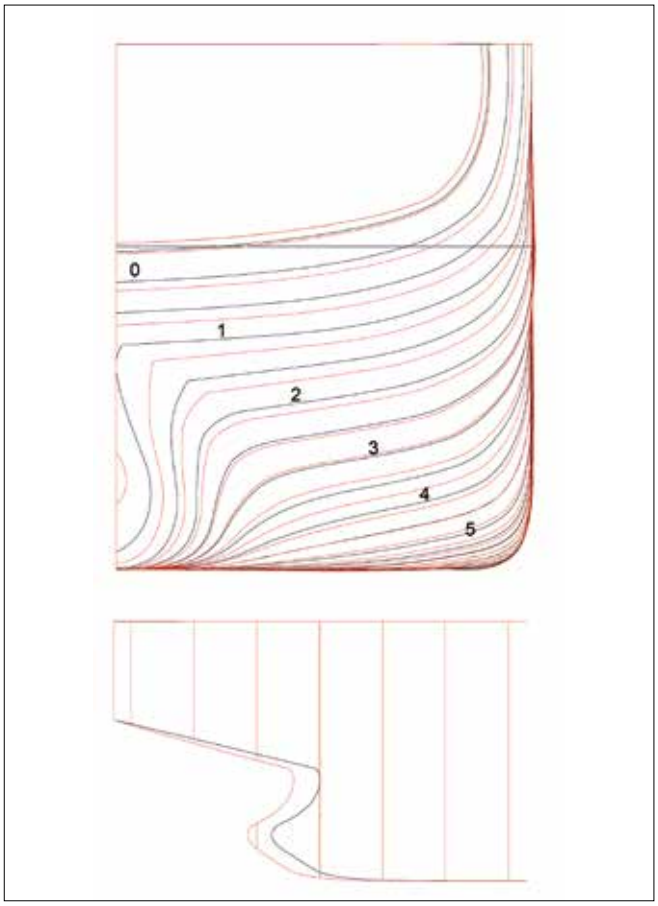

Fig. 24. Aft part - parent shape (black) vs. optimised one (red)

RESULTS OF EXPERIMENTAL VERIFICATION

The experiments were carried out on a model built at a scale 17.035, in the towing tank at CTO, S.A. The model was built in two parts, so that the influence of the bow part optimisation and stern part optimisation could be verified separately. Three configurations were tested:

– initial bow + initial stern
– optimised bow + optimised stern
– optimised bow + optimised stern.

The experimental model is presented in Fig. 25.

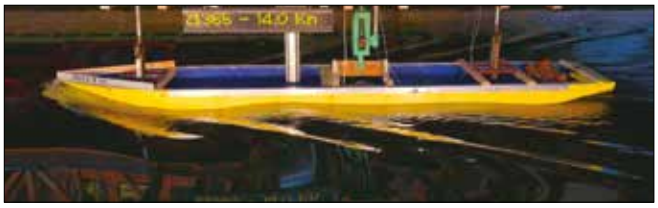

Fig. 25. Model testing

The resulting resistance (the direct results of the model tests) is presented in Fig. 26.

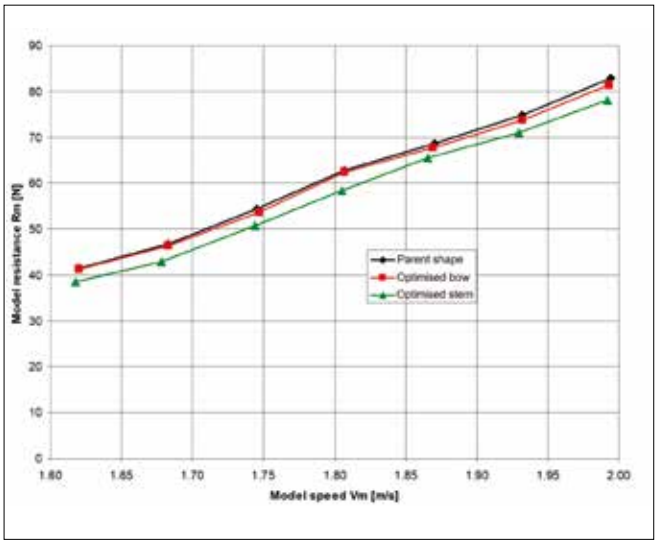

Fig. 26. Results of model tests

A quantitative comparison between the full scale resistance extrapolated from model tests and those computed with CFD for a design speed of 14 knots, is presented in Table 2.

Tab. 2. Comparison between model tests and CFD

	Experiment		CFD	
	Resist. [kN]	Reduct. [%]	Resist. [kN]	Reduct. [%]
Optim. Bow / orig. aft	211.4	–	183.4	–
Optim. Bow / orig. aft	207.9	1.7	178.7	2.5
Optim. Bow / orig. aft	200.8	5.0	176.8	3.6

A general underestimation of the total resistance in CFD computations can be observed, which is primarily explained by neglecting the dynamic trim and sinkage in CFD. Besides that, the resistance measurement results show different values of the gain in total resistance due to optimisation; however, the tendency observed in CFD computations was confirmed.

SUMMARY

This paper proposes an approach to parametric optimisation of a ship's hull, with respect to resistance, based on *a posteriori* transformation of an existing CAD file. The transformation is realised so that the volume of the submerged part remains unchanged. The optimisation is realised by coupling the CFD solver STAR-CCM+ with the NX CAD software. A prescribed set of parameters is considered and the resulting modifications are compared, with respect to total resistance. The bow part and the stern part were optimised separately. The conclusions are as follows:

– the parent shape is already well optimised, so that only a small reduction in resistance could be achieved;
– some reduction in resistance was obtained, both for the bow part and for the stern part (in the case of the bow part, the reduction in resistance was mainly achieved by bow bulb elongation);
– the values resulting from model testing are not consistent with the values obtained from CFD; however, the correct tendency was shown with CFD computations;
– the possibility of modification with the presented method is extremely limited, but, on the other hand, it can be applied quite fast and the optimisation process is relatively short, as the optimum can be found for a small number of variants.

Further work should include taking into account the following issues:

– introducing the constraints in the stern shape transformation, so that the propeller space remains unchanged;
– verification of the influence of stern shape transformation on propulsive and cavitation characteristics, based on a study similar to the one presented, e.g. by Zhang et al. [21].

ACKNOWLEDGEMENTS

This research was financed by the National Centre for Research and Development of the Republic of Poland, within the framework of the Esthetics project (POLTUR3/ESTHETICS/1/2019).

BIBLIOGRAPHY

1. Y. Lu, J. Wu, W. Li and Y. Wu, 'A new six-dof parallel mechanism for captive model test', Polish Maritime Research, No. 3 (107), Vol. 27; pp. 4-15, 2020, DOI: 10.2478/pomr-2020-0041 27.

2. S. Bielicki, 'Prediction of ship motions in irregular waves based on response amplitude operators evaluated experimentally in noise waves', Polish Maritime Research, No. 1(109), Vol. 28, pp. 16-27, 2021, DOI: 10.2478/pomr-2021-0002.

3. Q. Wang, P. Yu, B. Zhang, G. Li, 'Experimental Study and Numerical Simulation of the Water Entry of a Ship-Like Symmetry Section with an Obvious Bulbous Bow', Polish Maritime Research, No. 3(111), Vol. 28, pp. 16-34, 2021, DOI: 10.2478/pomr-2021-0031.

4. A. Karczewski, M. Kunicka, 'Influence of the Hull Shape on the Energy Demand of a Small Inland Vessel with Hybrid Propulsion', Polish Maritime Research, No. 3(111), Vol. 28, pp. 16-34, 2021, DOI: 10.2478/pomr-2021-0032.

5. H.C. Raven, 'A solution method for the nonlinear ship wave resistance problem', Ph.D. dissertation, Delft Univ. Techn., 1996.

6. A. Stück, 'Adjoint Navier-Stokes Methods for Hydrodynamic Shape Optimisation', Ph.D. dissertation, Technische Universitat Hamburg-Harburg, 2012.

7. M. Gundelach, 'Sketched Parametric Modeling in CFD Optimisation', Master thesis, Feb/2017, University of Rostock, Germany.

8. H. Nowacki, D. Liu, and X. Lü, 'Fairing bézier curves with constraints', Computer Aided Geometric Design, 7(1–4), 43–55 (1990).

9. S. Harries, 'Parametric Design and Hydrodynamic Optimisation of Ship Hull Forms', Mensch-und-Buch-Verlag, Berlin (1998).

10. S. Harries, C. Abt, 'Parametric curve design applying fairness criteria', International Workshop on Creating Fair and Shape-Preserving Curves and Surfaces (1998).

11. I. Biliotti, S. Brizzolara, M. Viviani, G. Vernengo, D. Ruscelli, M. Galliussi, D. Guadalupi, and A. Manfredini, 'Automatic parametric hull form optimisation of fast naval vessels', Proceedings of the Eleventh International Conference on Fast Sea Transportation (FAST 2011), 2011.

12. S. Han, Y.-S. Lee, and Y.B. Choi, 'Hydrodynamic hull form optimisation using parametric models', Journal of Marine Science and Technology, 17(1), 1–17, 2012, DOI: 10.1007/s00773-011-0148-8.

13. M. Brenner, V. Zagkas, S. Harries, and T. Stein, 'Optimisation using viscous flow computations for retrofitting ships in operation', Proceedings of the 5th International Conference on Computational Methods in Marine Engineering, MARINE, 2013.

14. Y. Feng, O. el Moctar, and T.E. Schellin, 'Parametric Hull Form Optimisation of Containerships for Minimum Resistance in Calm Water and in Waves', Journal of Marine Science and Application 20, 670–693, 2021. DOI: 10.1007/s11804-021-00243-w.

15. G. Vernengo, D. Villa, S. Gaggero, and M, Viviani, 'Interactive design and variation of hull shapes: pros and cons of different CAD approaches', International Journal on Interactive Design and Manufacturing, 14, pp. 103-114, 2020. DOI: 10.1007/s12008-019-00613-3.

16. D. Peri, and E.F. Campana, 'Multidisciplinary design optimisation of a naval surface combatant', Journal of Ship Research 47(1), 1–12, 2003, DOI: 10.5957/jsr.2003.47.1.1.

17. F. Perez, and J.A. Clemente, 'Constrained design of simple ship hulls with b-spline surfaces', Computer Aided Design 43(12), 1829–1840, 2011, DOI:10.1016/j.cad.2011.07.008.

18. H.J. Choi, 'Hull-form optimisation of a container ship based on bell-shaped modification function', International Journal of Naval Architecture and Ocean Engineering 7(3), 478–489, 2015, DOI: 10.1515/ijnaoe-2015-0034.

19. G.G. Lorentz, 'Bernstein Polynomials', University of Toronto Press, 1953.

20. H. Lackenby, 'On the systematic geometrical variation of ship forms', Trans. INA 92, 289–315, 1950.

21. Y. Zhang, X. P. Wu, M. Y. Lai, G. P. Zhou and J. Zhang, 'Feasibility Study of Rans in Predicting Propeller Cavitation in Behind-Hull Conditions', Polish Maritime Research, No. 4(108), Vol. 27, pp. 26-35, 2020, DOI: 10.2478/pomr-2020-0063.

CONTACT WITH THE AUTHOR

Marek Kraskowski
e-mail: marek.kraskowski@cto.gda.pl

Maritime Advanced Research Centre S.A.
Ship Hydromechanics Division
Gdansk
Poland